

pubs.acs.org/Macromolecules Article

# Nanobowls from Amphiphilic Core—Shell Cyclic Bottlebrush Polymers

Digvijayee Pal, John B. Garrison, Zhihui Miao, Lily E. Diodati, Adam S. Veige,\* and Brent S. Sumerlin\*



Cite This: https://doi.org/10.1021/acs.macromol.2c01232



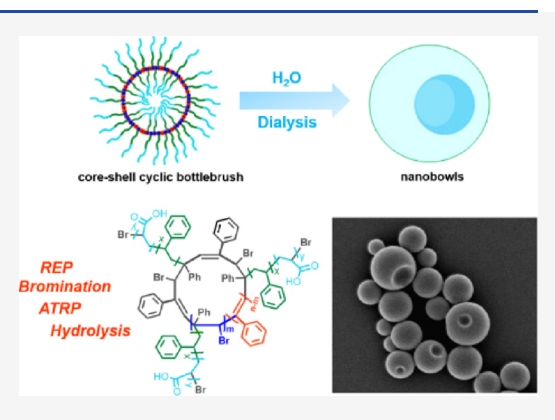
**ACCESS** I

III Metrics & More

Article Recommendations

Supporting Information

ABSTRACT: Cyclic bottlebrush polymers are macrocycles that contain pendent side-chain polymers on nearly every repeat unit. We leveraged a method to generate cyclic bottlebrush polymers utilizing ring-expansion polymerization (REP) followed by subsequent grafting-from via atom-transfer radical polymerization (ATRP) to produce core—shell cyclic bottlebrush polymers and investigated their self-assembly behavior in water. The bottlebrush polymers were comprised of a cyclic backbone with side chains composed of a hydrophobic polystyrene block and a hydrophilic poly(acrylic acid) block. A two-step morphological transformation from spheres to porous spheres to nanobowls (spheres with a single large pore) was observed with solvent exchange from tetrahydrofuran to water. In contrast, under identical experimental conditions, an analogous linear bottlebrush polymer with a similar backbone and side chain degrees of polymerizations did not aggregate into nanobowls but rather exhibited a porous sphere morphology. These



unusual morphologies and their propensities to transform can be attributed to changes in the internal viscosity of the aggregates during the solvent exchange process. Additionally, the rate of solvent exchange was found to influence the propensity for shape transformation to occur.

# ■ INTRODUCTION

Polymer composition and architecture greatly impact material properties and performance. The nuanced manipulation of these features has led to interesting polymer architectures that display both self-assembly and stimuli-responsive behavior, both of which find important applications in biomedicine. Cyclic polymers invite particular interest because of the unique properties this architecture displays relative to linear counterparts. The presence or absence of polymer chain ends plays a crucial role in chain dynamics such as chain mobility, hydrodynamic volume, and intrinsic viscosity. Cyclic polymer chains have less conformational freedom and experience inhibited mobility as compared to linear chains. Accompanying this decreased mobility are smaller hydrodynamic diameters, decreased intrinsic viscosity, and diminished responses and adaption to environmental stimuli.

Cyclic polymers are primarily produced using two different synthetic methods: (1) ring-closing, where functional moieties at the chain ends are coupled together via efficient ligation reactions,  $^{11-14}$  and (2) ring-expansion polymerization (REP), where a transition metal complex catalyst undergoes ring expansion.  $^{15-24}$  Because of the smaller hydrodynamic radius of cyclic polymers, they exhibit lower radii of gyration ( $R_g$ ) and intrinsic viscosities as compared to a linear polymer of the same composition and molecular weight. Thus, gel permeation chromatography (GPC) with light scattering detection and viscometry are the traditional methods for characterizing cyclic

polymers. However, both methods are indirect measurements and only support the presence of cyclic structures. In 2008, Deffieux and associates<sup>25</sup> proposed using atomic force microscopy (AFM) to directly visualize the cyclic topology of cyclic bottlebrush polymers. Cyclic bottlebrush polymers are complex macromolecular structures with polymer side chains densely grafted to a cyclic polymer backbone. So far, three synthetic pathways, namely, grafting-to,  $^{25-28}$  grafting-through,  $^{29,30}$  and grafting-from  $^{31-34}$  are utilized to install side chains on the cyclic backbone. In a previous report, we used a ring-expansion polymerization (REP) and a subsequent atom transfer radical polymerization (ATRP) grafting-from approach to prepare ultrahigh molecular weight cyclic bottlebrush polymers.<sup>35</sup> Several reports have shown that stimuli-responsive cyclic bottlebrush polymers exhibit improved efficacy in several drug delivery applications compared to their linear analogs. 34,36,37 Herein, we extend the REP-ATRP synthetic method to amphiphilic core-shell cyclic bottlebrush polymers for applications requiring more targeted outcomes.

Received: June 13, 2022 Revised: August 1, 2022



Scheme 1. Synthesis of Amphiphilic Core-Shell Cyclic Bottlebrush Polymers

Self-assembly of amphiphilic block copolymers in water via the solvent-exchange process is a widespread technique used to produce polymer aggregates with different morphologies, for example, micelles, worms, vesicles, and nanotubes. <sup>38–42</sup> Amphiphilic cyclic block copolymers have also been shown to self-assemble into micelles; <sup>3,4,43</sup> however, the size of the micelles is typically smaller and more compact, which confers stability to nanoparticles during loading with small molecule cargo and subsequent dilution. This is arguably an advantage over nanoparticles formed by linear amphiphilic block copolymers.

Although there are many reports on the self-assembly of linear amphiphilic bottlebrush polymers, thus far, the self-assembly of cyclic bottlebrush polymers has not been broadly explored. Deffieux and coworkers<sup>25</sup> found that cyclic bottlebrush polymers with random side chains of polystyrene and polyisoprene undergo self-assembly into nanotubes in the presence of solvents that were selective for polystyrene or polyisoprene. Wei and coworkers<sup>44</sup> noticed the formation of micelles when they explored the self-assembly of a cyclic bottlebrush polymer with heterogeneous amphiphilic polymer side chains derived from oligo( $\varepsilon$ -caprolactone) and oligo-(ethylene glycol). There remains a vast opportunity to discern the self-assembly behavior of this class of cyclic bottlebrush polymers.

In this work, we prepare and demonstrate the self-assembly of amphiphilic core—shell cyclic bottlebrush polymers for cyclic polyphenylacetylene (c-PPA) with amphiphilic block copolymer side chains of polystyrene (PS) and poly(acrylic acid) (PS-b-PAA) (Scheme 1). The cyclic PPA backbone and PS side chains serve as the hydrophobic core while the PAA block serves as the hydrophilic shell. Interestingly, these

polymers were found to self-assemble into unique nanobowl (spheres with a single large pore) morphologies in water. Additionally, an analogous linear amphiphilic core—shell bottlebrush polymer with a similar backbone and a side-chain degree of polymerization ( $\mathrm{DP_n}$ ) was synthesized via the same reaction protocol with an alternative catalyst. The linear analog did not aggregate into nanobowls but rather exhibited a porous sphere morphology. The aggregates were characterized by dynamic light scattering (DLS), static light scattering (SLS), transmission electron microscopy (TEM), and scanning electron microscopy (SEM) techniques.

### ■ RESULTS AND DISCUSSION

We prepared amphiphilic core-shell cyclic bottlebrush polymers using REP for the cyclic backbone and an ATRP grafting-from approach for the amphiphilic block copolymer side chains. Synthesis of c-PPA via REP is straightforward using the pincer ligand-supported tungsten catalyst developed by Veige and co-workers (Scheme 1). In our previous report, 35 we demonstrated a synthetic strategy to generate macrocyclic bottlebrush polymers following two simple steps using c-PPA as a scaffold: first, bromination of the olefinic double bonds of c-PPA and second, ATRP from the benzylic bromide positions of the resulting cyclic macroinitiator to grow different polymeric side chains. In this work, we followed the same protocol to first synthesize a cyclic bottlebrush polymer with polystyrene side chains (Scheme 1). Utilizing this polymer as a macroinitiator, the polystyrene block was chain extended with tert-butyl acrylate to form a poly(tert-butyl acrylate) (P<sup>t</sup>BA) block. Subsequent deprotection of the P<sup>t</sup>BA

segment produced the poly(acrylic acid) (PAA) block and the desired amphiphilic PS-b-PAA side chains (Scheme 1).

Characterization of c-PPA via GPC revealed a monomodal molecular weight distribution with a number average molecular weight  $(M_n)$  of 60 kDa  $(\mathrm{DP}_{n,c\text{-PPA}}=587)$  and a dispersity (D) of 1.52 (Figure S1). To aid in comparing the cyclic architecture to a linear counterpart, a linear PPA (l-PPA) was also synthesized using an acetylacetonato (1,5-cyclooctadiene)rhodium(I) catalyst in THF at ambient temperature. The resulting linear polymer showed an  $M_n$  of 62 kDa and a D of 1.51 (Figure S1). When comparing the plot of log(molar mass) versus elution time for c-PPA and l-PPA (Figure S2), it was clear that at any point along the elugram, c-PPA eluted later than its linear counterpart of identical molecular weight. These data support a smaller hydrodynamic diameter for c-PPA because of its cyclic topology.

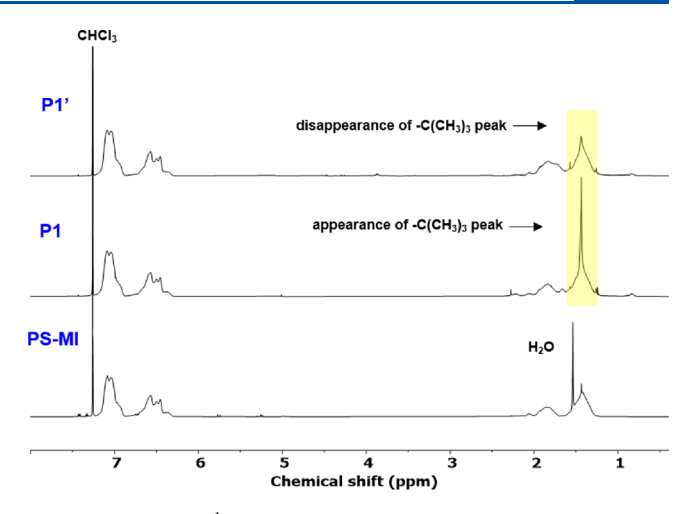
Electrophilic addition of excess  $Br_2$  to c-PPA produced the cyclic macroinitiator with brominated ATRP initiating sites on the benzylic positions along the polymer backbone (c-PPABr, Scheme 1). Characterization of c-PPABr via  $^1H$  NMR spectroscopy was inconclusive in determining bromine incorporation efficiency, as the methine signals overlapped with those from the aromatic protons (Figure S3). Therefore, elemental analysis was used to reveal that 54% of the alkenes were brominated in c-PPABr, and the  $M_n$  and D of the resulting polymers were 113 kDa and 1.85, respectively (Table 1).

Table 1. Results from Cyclic Polymerizations<sup>a</sup>

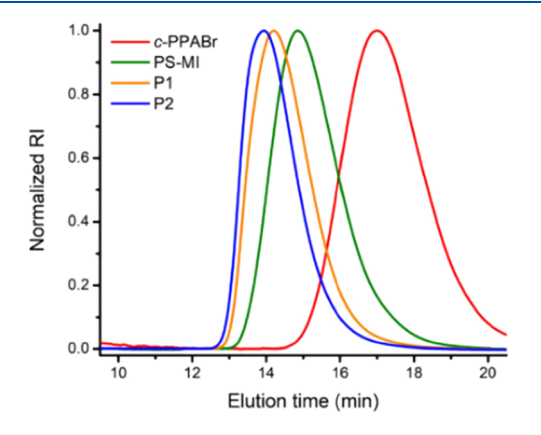
entry	conv. <sup>b</sup> (%)	$M_{\rm n,theo}^{c}~({\rm kDa})$	$M_{\rm n,GPC}^{}^{}$ (kDa)	Đ
c-PPABr		110	113	1.85
PS-MI	20	1950	1780	1.68
P1	3	2270	2150	1.67
P2	10	2850	2730	1.68

ac-PPABr: brominated cyclic polyphenylacetylene; PS-MI: cyclic bottlebrush polymers with polystyrene side chains (c-PPABr-g-PS); P1/P2: two examples of cyclic bottlebrush polymers with polystyrene-co-poly(tert-butyl acrylate) side chains (c-PPABr-g-(PS-b-P¹BA)).
bMonomer conversions were calculated via ¹H NMR spectroscopy using trioxane as an internal standard. <sup>c</sup>Theoretical number-average molecular weight of the cyclic bottlebrush polymers. <sup>d</sup>Absolute number-average molecular weight determined by gel permeation chromatography equipped with a multi-angle light scattering detector.

Polystyrene side chains were then grafted from the macroinitiator c-PPABr via ATRP by using a CuBr/PMDETA (N,N,N',N'',N'')-pentamethyldiethylenetriamine) catalyst/ligand system and styrene monomer. 35 1H NMR spectroscopy of the resulting polymer c-PPABr-g-PS (PS-MI) revealed only the characteristic polystyrene protons without any detectable backbone protons (Figure 1). This was not surprising as signals for protons in the cyclic backbone are obscured by those for protons in the polystyrene side chains. Similarly, the <sup>13</sup>C NMR spectrum of PS-MI (Figure S4) evidenced only the characteristic polystyrene side chain carbon signals. However, the <sup>13</sup>C NMR spectrum did reveal a complete disappearance of the C-Br carbon peak at ~68 ppm. Only the characteristic polystyrene carbons were observed without any backbone alkene and phenyl carbons being visible, consistent with the fact that the newly grown polystyrene side chains overwhelm and obscure the backbone signals. GPC analysis (Figure 2,



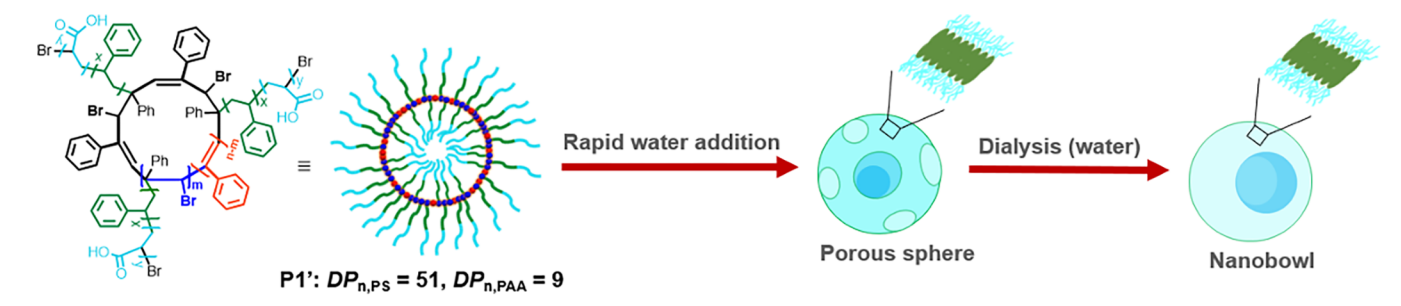
**Figure 1.** Overlaid <sup>1</sup>H NMR spectra of cyclic bottlebrush polymers with polystyrene side chains (**PS-MI**), polystyrene-*co*-poly(*tert*-butyl acrylate) side chains (**P1**), and polystyrene-*co*-poly(acrylic acid) side chains (**P1**'). Appearance of a sharp signal at 1.46 ppm originated from the  $-C(CH_3)_3$  protons suggested successful poly(*tert*-butyl acrylate) chain extension from **PS-MI**, while disappearance of the same peak upon acidic work-up indicated successful poly(acrylic acid) block formation due to deprotection.



**Figure 2.** GPC traces of brominated cyclic polyphenylacetylene (*c*-**PPABr**), cyclic bottlebrush polymers with polystyrene side chains (**PS-MI**), and polystyrene-*b*-poly(*tert*-butyl acrylate) side chains (**P1**/**P2**). GPC was performed by using DMAc with 50 mM LiCl as a mobile phase at 50 °C.

Table 1) of the PS-MI indicated an  $M_{\rm n}$  of 1780 kDa and a  $\mathcal D$  of 1.68. Additionally, this molecular weight showed good agreement with the theoretical  $M_{\rm n}$  (1950 kDa) of the cyclic bottlebrush polymer calculated based on the monomer conversions and polymerization stoichiometry. Dispersity of the resulting bottlebrush polymers remained almost equivalent to the macroinitiator, which is expected for a bottlebrush polymer prepared using a grafting from approach.

The polystyrene block of **PS-MI** was then chain extended with *tert*-butyl acrylate via ATRP to generate a precursor to the amphiphilic block copolymer side chains. We utilized the active initiating sites present at the polystyrene chain ends to target two different average degrees of polymerization (DP<sub>n</sub>) of the P<sup>t</sup>BA block of 9 and 23. These two cyclic bottlebrush polymers (*c*-**PPABr**-*g*-(**PS**-*b*-**P**<sup>t</sup>BA)) were named **P1** and **P2**, respectively. <sup>1</sup>H NMR spectroscopy of the polymers revealed successful side chain extension by the appearance of a sharp peak at 1.46 ppm, indicative of the  $-C(CH_3)_3$  protons on the



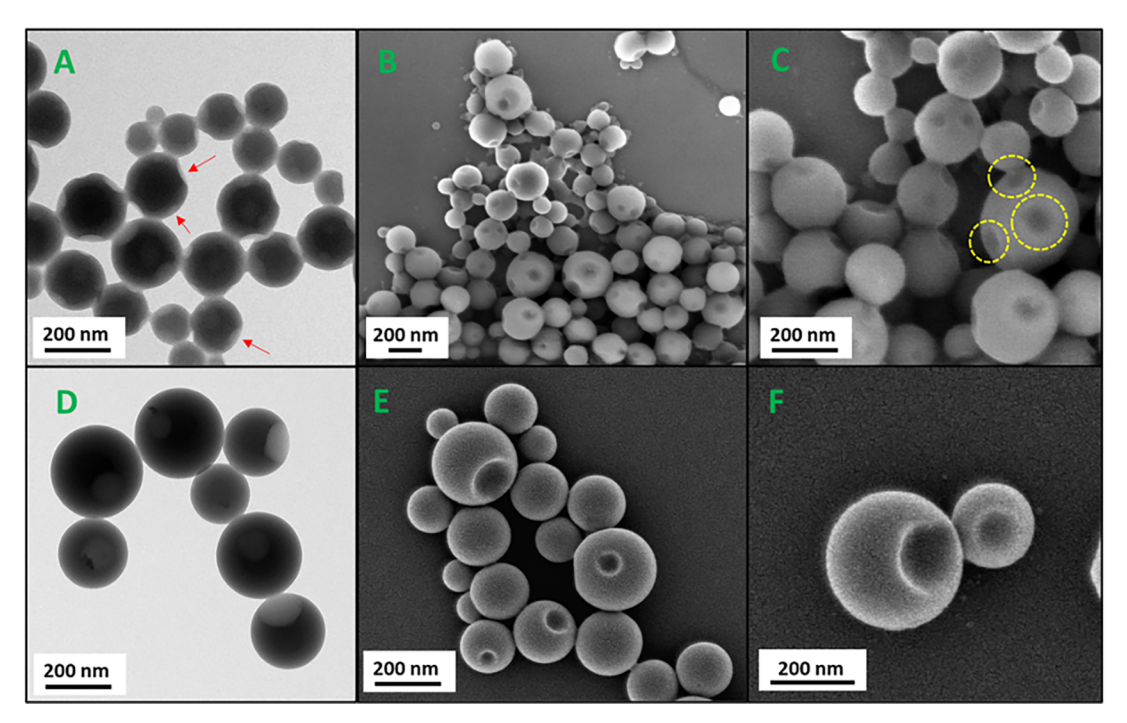


Figure 3. Proposed mechanism of the formation of the porous spheres and nanobowls upon self-assembly of the cyclic bottlebrush polymers in DI water. TEM (A) and SEM (B,C) images of the porous spheres produced from the polymer P1' ( $DP_{n,PS} = 51$ ,  $DP_{n,PAA} = 9$ ). TEM (D) and SEM (E,F) images of the nanobowls produced from the polymer P1'.

P<sup>t</sup>BA block (Figures 1 and S5). As expected, the molecular weights of the initial PS-MI polymers increased to 2150 and 2730 kDa for P1 and P2, respectively, demonstrating successful chain extension. The dispersity of P1 and P2 remained consistent with PS-MI as per GPC analysis (Table 1, Figure 2). Deprotection of the P<sup>t</sup>BA blocks of P1 and P2 to hydrophilic PAA blocks was executed by treating the polymers with trifluoroacetic acid (Scheme 1) resulting in two amphiphilic core—shell cyclic bottlebrush polymers (*c*-PPABr-*g*-(PS-*b*-PAA)), P1' and P2', respectively. <sup>1</sup>H NMR spectroscopy of P1' and P2' offered evidence of a clear disappearance of the sharp -C(CH<sub>3</sub>)<sub>3</sub> proton signals at 1.46 ppm (Figures 1 and S5), confirming successful deprotection of the P<sup>t</sup>BA blocks.

Once we synthesized the amphiphilic core—shell cyclic bottlebrush polymers P1' and P2', we explored their self-assembly behavior in aqueous media. Complementary characterization techniques of DLS, SLS, TEM, and SEM revealed how these polymers behaved during a solvent exchange process with THF and deionized (DI) water. As DI water is a poor solvent for the polystyrene blocks, we expect to see self-assembly during the transition from THF. Polymers P1' (DP<sub>n,PS</sub> = 51, DP<sub>n,PAA</sub> = 9) and P2' (DP<sub>n,PS</sub> = 51, DP<sub>n,PAA</sub> = 23) were first independently dissolved in THF (1 mg/mL).

DLS experiments on the optically clear polymer solution of P1' in THF exhibited an initial hydrodynamic diameter  $(D_h)$ of 28 nm (Figure S6). DI water (4 mL) was then added dropwise into the polymer solutions. With the addition of water, the clear solutions of dissolved P1' and P2' gradually transformed to suspended cloudy solutions, suggesting some degree of polymer aggregation. DLS of P1' particles present in the cloudy solution revealed a  $D_h$  of 415 nm (Figure S6), consistent with the self-assembly of the polymer in the presence of water. Furthermore, SLS experiments (Figure S7) provided information about the spatial density distribution and morphology of these nanoparticles. The value of the  $R_{\rm g}/R_{\rm h}$ ratio was 1.06, which offered evidence for the formation of hollow solvent-swollen spherical particles.<sup>47</sup> TEM and SEM provided direct visualization of the P1' polymer aggregates. The images revealed porous nanospheres with diameters ranging from 100 to 250 nm (Figure 3A-C). As expected, these diameters are smaller than the  $D_h$  obtained from DLS analysis, as TEM and SEM analyses are dry state measurements. Interestingly, further increasing the water content of the P1' solution by dialyzing for 48 h caused an additional shape transformation. The multi-porous spheres transitioned to particles with a single pore, as shown through TEM (Figure 3D) and SEM analysis (Figure 3E, F). These types of

structures are often described as nanobowls or stomatocytes.  $^{48-52}$  Typically, this unique morphology is a consequence of a very long hydrophobic block relative to the hydrophilic block.  $^{48-52}$  Increasing the PAA block length of the amphiphilic side chains in P2' (DP<sub>n,PAA</sub> = 23) resulted in similar self-assembled morphologies (Figures S7–S9). The proposed mechanism of self-assembly during solvent exchange from THF to water is outlined in Figure 4. Self-assembly of the

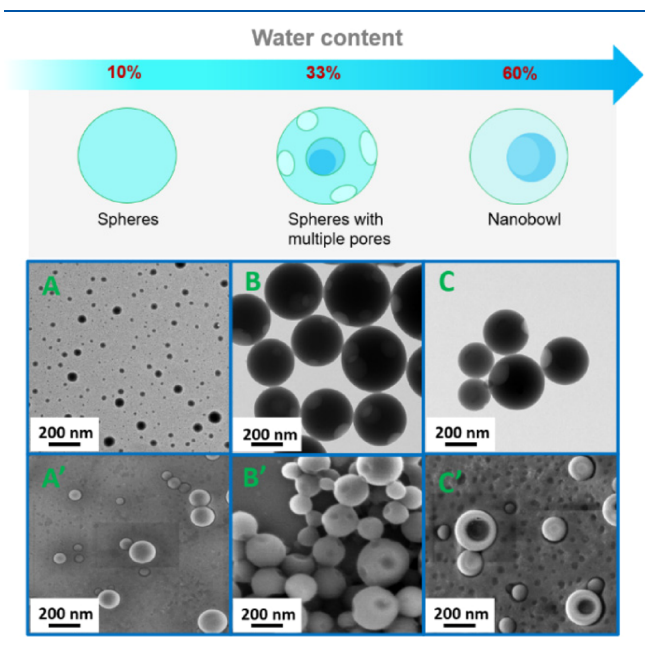


**Figure 4.** (top) Proposed schematic representation of nanobowl formation where increased % water content leads to a morphological change from spheres to porous spheres and finally to nanobowls, as the pores coalesce into one large void. (A-C) TEM and (A'-C') SEM images of the nanoparticles at different % water content.

amphiphilic core-shell cyclic polymers into spherical nanoparticles occurs as the hydrophobic polystyrene blocks and cyclic backbone collapse on themselves and are shielded by the hydrophilic PAA blocks during the gradual addition of water. We reasoned that when the water content was low, the interior of the aggregates remains partially solvated by the nonselective THF, while the exterior of the sphere is soft due to hydration. The solvent-aided mobility within the particle interior leads to rapid solvent diffusion in and out of the soft skin and homogeneous collapse of the spheres. Continuous addition of water leads to the displacement of THF from the core of the aggregates. Further collapse of the hydrophobic regions leads to an increase in internal viscosity and possible hardening of the skin. The confined droplets formed inside the aggregates during water addition start to coalesce to form larger droplets. Upon further addition of water, the organic solvent in the interior droplets diffuses out faster than the rate at which water diffuses in, leading to pore creation. A difference in hydrostatic pressure is thus created where the pressure is lower on the inside. The pores then coalesce, and while the pressure difference is presumably equal throughout the aggregate, a thin portion of the wall is vulnerable to an inward break-through, which results in the formation of the opening of the bowl. Nanobowls are, therefore, the consequence of shape transformation from spheres during the solvent exchange process. As stated above, this morphology usually forms when the hydrophobic block is considerably longer than the hydrophilic

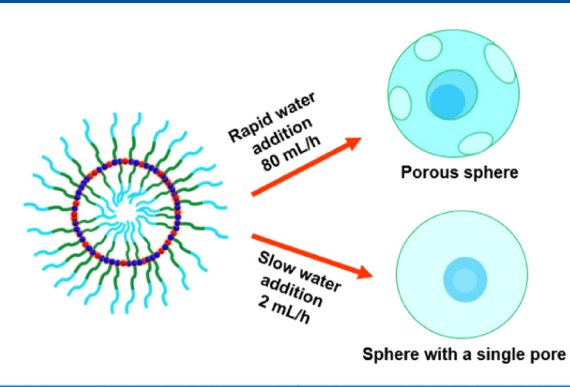
block.  $^{48-52}$  In the case of the amphiphilic core—shell cyclic bottlebrush polymers P1' and P2', the hydrophobic segments include the PPA backbone (DP<sub>n</sub> = 587) and the polystyrene blocks of the side chains (DP<sub>n</sub> = 51), which combined are much longer than the hydrophilic PAA blocks (DP<sub>n</sub> = 9 and 23, respectively). Overall, the hydrophobic character of P1' and P2' is nearly 90%.

Because the amphiphilic cyclic bottlebrush polymers have such interesting self-assembly behavior during solvent exchange, the relationship between the water content in the polymer solution, nanoparticle morphology, and propensity for shape transformation was interrogated. Accordingly, we conducted a systematic study to elucidate the morphological evolution that occurs during the addition of water. We began with a solution of P1' (1 mg/mL) in THF and added DI water dropwise to achieve a water content of 10%. This solution was directly analyzed by both TEM and SEM, which revealed the formation of spheres, as expected (Figure 4A and A'). In contrast with our initial solvent-exchange study, we did not dialyze these samples. Increasing the water content to 33% led to the formation of porous spheres, as confirmed by TEM and SEM analysis (Figure 4B and B'). Further increasing the water content to 60% generated nanobowls (Figure 4C and C'), while further addition of water did not result in a change in the nanobowl morphology for P1'. These results suggest that ~60% water content is needed to produce the nanobowls and that nanoparticle morphology can be controlled by tailoring the water content.

There may also be a kinetic component to the self-assembly process, and the rate of solvent exchange may affect the mechanism of shape transitions. We hypothesized that fast water addition would not provide enough time for the THF droplets to coalesce into a single large droplet, a more thermodynamically favorable process, because the hydrophobic segments would collapse and harden quickly. The trapped THF would instead be expected to bore random paths of escape out of the sphere. As a result, faster water addition would lead to porous spheres while a slower rate of water addition would generate nanobowls. To test this hypothesis, the water content was first fixed to 71% (i.e., 5 mL of DI water was added to 2 mL of a polymer/THF solution) for P1' and P2'. As anticipated, adding water at a rate of 80 mL/h resulted in nanoparticles that were porous spheres (Figure 5A). In contrast, adding water more slowly at a rate of 2 mL/h led to nanobowls (Figure 5B).

Once insight into the self-assembly behavior of the cyclic amphiphilic bottlebrush polymers was established, the role of backbone architecture was examined. Thus, an analogous linear amphiphilic core—shell bottlebrush polymer with a linear PPA backbone and PS-b-PAA side chains (*l*-PPABr-g-(PS-b-PAA)) (Figure 6) was synthesized following the same synthetic protocol as the cyclic polymer, but using a catalyst known for synthesizing linear polyphenylacetylene. 45,46

The  $M_n$  of the linear backbone (62 kDa) and DP<sub>n</sub> of the PS and PAA blocks (DP<sub>n,PS</sub> = 52 and DP<sub>n,PAA</sub> = 8) were almost identical to that of the cyclic bottlebrush polymer, **P1**′ (Figure 6A). Consistent with a previous report, adding bromine resulted in 72% bromination of backbone double-bonds in the case of the *l*-**PPA**. Gradual shifts of GPC traces toward higher molecular weight (Figure 6A) suggested successful side chain polymerization of styrene from the linear brominated macroinitiator (*l*-**PPABr**) and subsequent chain extension with *tert*-butyl acrylate from the resulting linear bottlebrush polymer



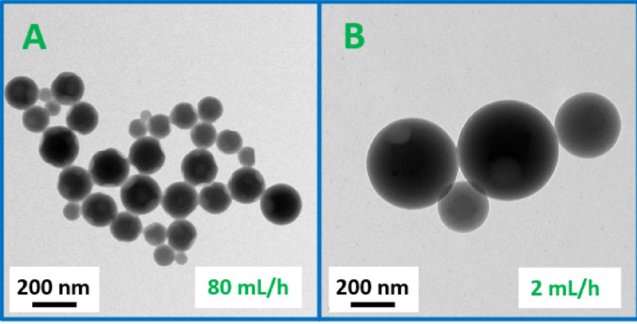


**Figure 5.** (Top) Proposed effect of the rate of water addition on particle morphology. (A) TEM image of the nanoparticles showing spheres with multiple pores generated from the fast water addition rate of 80 mL/h. (B) TEM image of the nanoparticles showing spheres with a single pore generated from the slow water addition rate of 2 mL/h.

with PS side chains (*l*-PPABr-*g*-PS). To observe its self-assembly behavior in water, 1 mg of the polymer was first

dissolved in 1 mL of THF, and then, 4 mL of water was added dropwise. TEM of the resulting cloudy solution revealed porous spherical nanoparticles with  $D_h$  of ~620 nm (Figure S10). Porous spheres with diameters ranging from 220 to 400 nm were observed by SEM (Figure 6B). Interestingly, even after 48 h of dialysis, the porous morphology remained intact, and no nanobowl formation was observed. The differences in morphological evolution during self-assembly is potentially attributable to the difference in backbone mobility that arises from varying the architecture<sup>53</sup> (i.e., linear vs cyclic) and differing degrees of backbone bromination (linear = 72% vs cyclic = 54%). Differences in mobility between the two brush architectures may also explain the differences observed in the thermal and mechanical stability of the nanoparticles formed by the cyclic and linear bottlebrush polymers during heating and sonication (Figures S11-S13).

#### CONCLUSIONS

We established a synthetic strategy to generate amphiphilic core—shell cyclic bottlebrush polymers using a tandem REP and grafting-from ATRP process. Self-assembly of amphiphilic core—shell cyclic bottlebrush polymers in water was observed during solvent exchange from THF to water to reveal an unusual nanobowl morphology. We attribute this shape transformation to a change in the internal viscosity of the nanoparticles during the solvent exchange process, where smaller solvent droplets coalesce to one pore. To study the influence of backbone architecture, we investigated the self-assembly of an analogous linear bottlebrush polymer. Interestingly, under identical conditions, a shape transformation from spheres to porous spheres was observed for the linear bottlebrush polymer, with no subsequent transformation to nanobowls. These results suggest that control

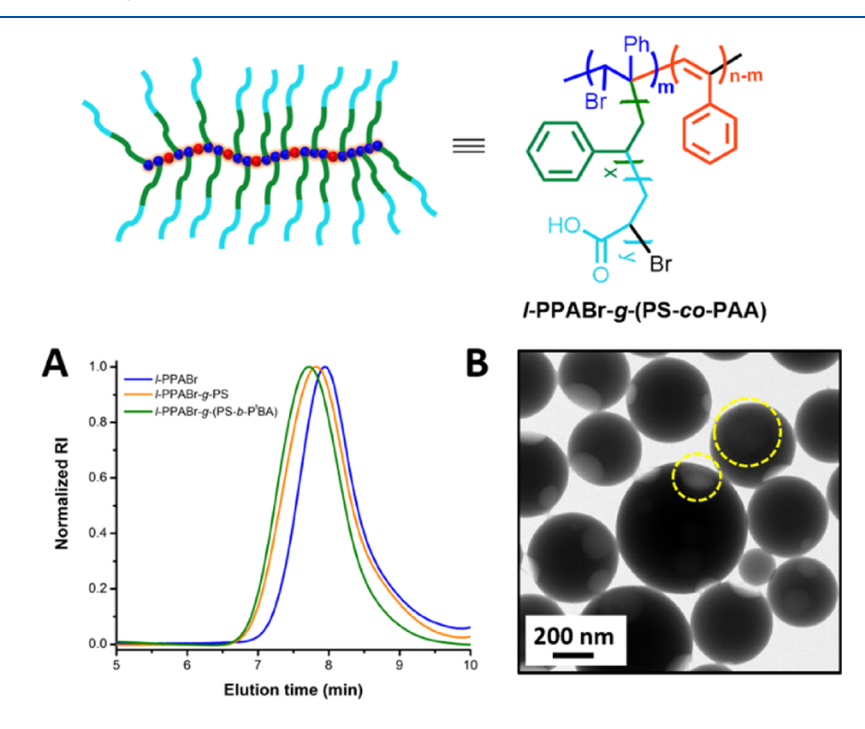


**Figure 6.** (Top) Structure of a linear amphiphilic core—shell bottlebrush polymer. (A) GPC traces of brominated linear polyphenylacetylene (*I*-**PPABr**), linear bottlebrush polymers with polystyrene side chains (*I*-**PPABr-g-(PS-co-P'BA)**). Absolute number-average molecular weight determined by gel permeation chromatography (GPC) equipped with a multiangle light scattering detector and using THF as a mobile phase at 35 °C. (B) TEM image of porous spheres of the amphiphilic core—shell linear bottlebrush polymer in water.

over backbone architecture can be harnessed to direct the self-assembly behavior of core—shell bottlebrushes.

# ASSOCIATED CONTENT

## **Solution** Supporting Information

The Supporting Information is available free of charge at https://pubs.acs.org/doi/10.1021/acs.macromol.2c01232.

Full experimental procedures, NMR spectra, GPC data and AFM data (PDF)

### AUTHOR INFORMATION

# **Corresponding Authors**

Adam S. Veige — George & Josephine Butler Polymer Research Laboratory, Center for Macromolecular Science & Engineering, Department of Chemistry and Center for Catalysis, Department of Chemistry, University of Florida, Gainesville, Florida 32611, United States; ocid.org/ 0000-0002-7020-9251; Email: veige@chem.ufl.edu

Brent S. Sumerlin — George & Josephine Butler Polymer Research Laboratory, Center for Macromolecular Science & Engineering, Department of Chemistry, University of Florida, Gainesville, Florida 32611, United States; orcid.org/ 0000-0001-5749-5444; Email: sumerlin@chem.ufl.edu

#### **Authors**

- Digvijayee Pal George & Josephine Butler Polymer Research Laboratory, Center for Macromolecular Science & Engineering, Department of Chemistry, University of Florida, Gainesville, Florida 32611, United States
- John B. Garrison George & Josephine Butler Polymer Research Laboratory, Center for Macromolecular Science & Engineering, Department of Chemistry, University of Florida, Gainesville, Florida 32611, United States
- Zhihui Miao George & Josephine Butler Polymer Research Laboratory, Center for Macromolecular Science & Engineering, Department of Chemistry and Center for Catalysis, Department of Chemistry, University of Florida, Gainesville, Florida 32611, United States
- Lily E. Diodati George & Josephine Butler Polymer Research Laboratory, Center for Macromolecular Science & Engineering, Department of Chemistry, University of Florida, Gainesville, Florida 32611, United States

Complete contact information is available at: https://pubs.acs.org/10.1021/acs.macromol.2c01232

## Funding

This material is based upon work supported by the National Science Foundation (CHE-2108266).

#### Notes

The authors declare no competing financial interest.

## ACKNOWLEDGMENTS

We acknowledge Prof. Daniel A. Savin for assistance with light scattering of the polymeric nanoparticle assemblies.

#### REFERENCES

- (1) Topological polymer chemistry: Progress of cyclic polymers in syntheses, properties, and functions, 1st ed.; Tezuka, Y., Ed.; World Scientific, 2013.
- (2) Laurent, B. A.; Grayson, S. M. Synthetic approaches for the preparation of cyclic polymers. *Chem. Soc. Rev.* **2009**, *38*, 2202.

- (3) Haque, F. M.; Grayson, S. M. The synthesis, properties and potential applications of cyclic polymers. *Nat. Chem.* **2020**, *12*, 433–444
- (4) Lienard, R.; De Winter, J.; Coulembier, O. Cyclic polymers: Advances in their synthesis, properties, and biomedical applications. *J. Polym. Sci.* **2020**, *58*, 1481–1502.
- (Ś) Beckham, H. W. Ring Polymers: Effective Isolation and Unique Properties. In *Complex Macromolecular Architectures*; Hadjichristidis, N., Hirao, A., Tezuka, Y., Du Prez, F., Eds.; John Wiley & Sons (Asia) Pte Ltd.: Singapore, 2011; pp 791–821.
- (6) Roovers, J. Organic cyclic polymers. In *Cyclic Polymers*; Springer, 2000; pp 347–384.
- (7) Jeong, Y.; Jin, Y.; Chang, T.; Uhlik, F.; Roovers, J. Intrinsic Viscosity of Cyclic Polystyrene. *Macromolecules* **2017**, *50*, 7770–7776.
- (8) Williams, R. J.; Dove, A. P.; O'Reilly, R. K. Self-assembly of cyclic polymers. *Polym. Chem.* **2015**, *6*, 2998–3008.
- (9) Nam, S.; Leisen, J.; Breedveld, V.; Beckham, H. W. Dynamics of unentangled cyclic and linear poly(oxyethylene) melts. *Polymer* **2008**, 49, 5467–5473.
- (10) Gartner, T. E., III; Haque, F. M.; Gomi, A. M.; Grayson, S. M.; Hore, M. J. A.; Jayaraman, A. Scaling exponent and effective interactions in linear and cyclic polymer solutions: Theory, simulations, and experiments. *Macromolecules* **2019**, *52*, 4579–4589.
- (11) Josse, T.; de Winter, J.; Gerbaux, P.; Coulembier, O. Cyclic Polymers by Ring-Closure Strategies. *Angew. Chem., Int. Ed.* **2016**, *55*, 13944–13958.
- (12) Laurent, B. A.; Grayson, S. M. An efficient route to well-defined macrocyclic polymers via "click" cyclization. *J. Am. Chem. Soc.* **2006**, 128, 4238–4239.
- (13) Touris, A.; Hadjichristidis, N. Cyclic and multiblock polystyrene-block-polyisoprene copolymers by combining anionic polymerization and azide/alkyne "click" chemistry. *Macromolecules* **2011**, *44*, 1969–1976.
- (14) Sun, P.; Chen, J.; Liu, J.; Zhang, K. Self-Accelerating Click Reaction for Cyclic Polymer. *Macromolecules* **2017**, *50*, 1463–1472.
- (15) Chang, Y. A.; Waymouth, R. M. Recent progress on the synthesis of cyclic polymers via ring-expansion strategies. *J. Polym. Sci., Part A: Polym. Chem.* **2017**, *55*, 2892–2902.
- (16) Bielawski, C. W.; Benitez, D.; Grubbs, R. H. An "endless" route to cyclic polymers. *Science* **2002**, *297*, 2041–2044.
- (17) Miao, Z.; Pal, D.; Niu, W.; Kubo, T.; Sumerlin, B. S.; Veige, A. S. Cyclic poly(4-methyl-1-pentene): Efficient catalytic synthesis of a transparent cyclic polymer. *Macromolecules* **2020**, *53*, 7774–7782.
- (18) Xia, Y.; Boydston, A. J.; Yao, Y.; Kornfield, J. A.; Gorodetskaya, I. A.; Spiess, H. W.; Grubbs, R. H. Ring-expansion metathesis polymerization: catalyst-dependent polymerization profiles. *J. Am. Chem. Soc.* **2009**, *131*, 2670–2677.
- (19) Roland, C. D.; Li, H.; Abboud, K. A.; Wagener, K. B.; Veige, A. S. Cyclic polymers from alkynes. *Nat. Chem.* **2016**, *8*, 791–796.
- (20) Nadif, S. S.; Kubo, T.; Gonsales, S. A.; VenkatRamani, S.; Ghiviriga, I.; Sumerlin, B. S.; Veige, A. S. Introducing "ynene" metathesis: ring-expansion metathesis polymerization leads to highly cis and syndiotactic cyclic polymers of norbornene. *J. Am. Chem. Soc.* **2016**, 138, 6408–6411.
- (21) Gonsales, S. A.; Kubo, T.; Flint, M. K.; Abboud, K. A.; Sumerlin, B. S.; Veige, A. S. Highly tactic cyclic polynorbornene: stereoselective ring expansion metathesis polymerization of norbornene catalyzed by a new tethered tungsten-alkylidene catalyst. *J. Am. Chem. Soc.* **2016**, *138*, 4996–4999.
- (22) Niu, W. J.; Gonsales, S. A.; Kubo, T.; Bentz, K. C.; Pal, D.; Savin, D. A.; Sumerlin, B. S.; Veige, A. S. Polypropylene: now available without chain ends. *Chem* **2019**, *5*, 237–244.
- (23) Miao, Z.; Gonsales, S. A.; Ehm, C.; Mentink-Vigier, F.; Bowers, C. R.; Sumerlin, B. S.; Veige, A. S. Cyclic polyacetylene. *Nat. Chem.* **2021**. *13*. 792–799.
- (24) Miao, Z.; Kubo, T.; Pal, D.; Sumerlin, B. S.; Veige, A. S. pH-responsive water-soluble cyclic polymer. *Macromolecules* **2019**, 52, 6260–6265.

- (25) Schappacher, M.; Deffieux, A. Synthesis of macrocyclic copolymer brushes and their self-assembly into supramolecular tubes. *Science* **2008**, 319, 1512–1515.
- (26) Lahasky, S. H.; Serem, W. K.; Guo, L.; Garno, J. C.; Zhang, D. Synthesis and characterization of cyclic brush-like polymers by *N*-heterocyclic carbene-mediated zwitterionic polymerization of *N*-propargyl *N*-carboxyanhydride and the grafting-to approach. *Macromolecules* **2011**, *44*, 9063–9074.
- (27) Zhang, K.; Lackey, M. A.; Wu, Y.; Tew, G. N. Universal cyclic polymer templates. *J. Am. Chem. Soc.* **2011**, *133*, 6906–6909.
- (28) Zhang, K.; Zha, Y.; Peng, B.; Chen, Y.; Tew, G. N. Metallo-supramolecular cyclic polymers. *J. Am. Chem. Soc.* **2013**, *135*, 15994–15997.
- (29) Boydston, A. J.; Holcombe, T. W.; Unruh, D. A.; Frechet, J. M. J.; Grubbs, R. H. A direct route to cyclic organic nanostructures via ring-expansion metathesis polymerization of a dendronized macromonomer. *J. Am. Chem. Soc.* **2009**, *131*, 5388–5389.
- (30) Xia, Y.; Boydston, A. J.; Grubbs, R. H. Synthesis and direct imaging of ultrahigh molecular weight cyclic brush polymers. *Angew. Chem., Int. Ed.* **2011**, *50*, 5882–5885.
- (31) Zhang, S.; Yin, L.; Zhang, W.; Zhang, Z.; Zhu, X. Synthesis of diverse cyclic-brush polymers with cyclic polystyrene as a universal template *via* a grafting-from approach. *Polym. Chem.* **2016**, 7, 2112–2120
- (32) Zhang, K.; Tew, G. N. Cyclic brush polymers by combining ring-expansion metathesis polymerization and the "grafting from" technique. *ACS Macro Lett.* **2012**, *1*, 574–579.
- (33) Fan, X.; Wang, G.; Huang, J. Synthesis of macrocyclic molecular brushes with amphiphilic block copolymers as side chains. *J. Polym. Sci., Part A: Polym. Chem.* **2011**, 49, 1361–1367.
- (34) Wei, H.; Chu, D. S. H.; Zhao, J.; Pahang, J. A.; Pun, S. H. Synthesis and evaluation of cyclic cationic polymers for nucleic acid delivery. *ACS Macro Lett.* **2013**, *2*, 1047–1050.
- (35) Pal, D.; Miao, Z.; Garrison, J. B.; Veige, A. S.; Sumerlin, B. S. Ultra-high-molecular-weight macrocyclic bottlebrushes via post-polymerization modification of a cyclic polymer. *Macromolecules* **2020**, 53, 9717–9724.
- (36) Tu, X. Y.; Meng, C.; Wang, Y. F.; Ma, L. W.; Wang, B. Y.; He, J. L.; Ni, P. H.; Ji, X. L.; Liu, M. Z.; Wei, H. Fabrication of thermosensitive cyclic brush copolymer with enhanced therapeutic efficacy for anticancer drug delivery. *Macromol. Rapid Commun.* **2018**, 39, No. 1700744.
- (37) Wang, C. E.; Wei, H.; Tan, N.; Boydston, A. J.; Pun, S. H. Sunflower polymers for folate-mediated drug delivery. *Biomacromolecules* **2016**, *17*, 69–75.
- (38) Zhulina, E. B.; Adam, M.; Larue, I.; Sheiko, S. S.; Rubinstein, M. Diblock copolymer micelles in a dilute solution. *Macromolecules* **2005**, *38*, 5330–5351.
- (39) Jain, S.; Bates, F. S. Consequences of nonergodicity in aqueous binary PEO–PB micellar dispersions. *Macromolecules* **2004**, *37*, 1511–1523.
- (40) Mai, Y.; Eisenberg, A. Self-assembly of block copolymers. *Chem. Soc. Rev.* **2012**, *41*, 5969–5985.
- (41) Liu, G. Block copolymer nanotubes derived from self-assembly. In *Self-assembled nanomaterials II*; Shimizu, T., Ed.; Advances in Polymer Science, vol 220; Springer: Berlin, Heidelberg, 2008; pp 29–64
- (42) Liu, X.; Gitsov, I. Nonionic amphiphilic linear dendritic copolymers, Morphology tuning by solvent-induced self-assembly. *Macromolecules* **2019**, *52*, 5563–5573.
- (43) Zhang, B.; Zhang, H.; Li, Y.; Hoskins, J. N.; Grayson, S. M. Exploring the effect of amphiphilic polymer architecture: synthesis, characterization, and self-assembly of both cyclic and linear poly(ethylene gylcol)-b-polycaprolactone. *ACS Macro Lett.* **2013**, *2*, 845–848.
- (44) Liu, Z.; Huang, Y.; Zhang, X.; Tu, X.; Wang, M.; Ma, L.; Wang, B.; He, J.; Ni, P.; Wei, H. Fabrication of cyclic brush copolymers with heterogeneous amphiphilic polymer brushes for controlled drug release. *Macromolecules* **2018**, *51*, 7672–7679.

- (45) Mastrorilli, P.; Nobile, C. F.; Rizzuti, A.; Suranna, G. P.; Acierno, D.; Amendola, E. Polymerization of phenylacetylene and of p-tolylacetylene catalyzed by  $\beta$ -dioxygenato rhodium(I) complexes in homogeneous and heterogeneous phase. *J. Mol. Catal. A: Chem.* **2002**, 178, 35–42.
- (46) Trhlíkova, O.; Zedník, J.; Balcar, H.; Brus, J.; Sedláček, J. [Rh(cycloolefin)(acac)] complexes as catalysts of polymerization of aryl- and alkylacetylenes: Influence of cycloolefin ligand and reaction conditions. *J. Mol. Catal. A: Chem.* **2013**, 378, 57–66.
- (47) McCallum, N. C.; Son, F. A.; Clemons, T. D.; Weigand, S. J.; Gnanasekaran, K.; Battistella, C.; Barnes, B. E.; Abeyratne-Perera, H.; Siwicka, Z. E.; Forman, C. J.; Zhou, X.; Moore, M. H.; Savin, D. A.; Stupp, S.; Wang, Z.; Vora, G. J.; Johnson, B. J.; Farha, O. K.; Gianneschi, N. C. J. Am. Chem. Soc. 2021, 143, 4005–4016.
- (48) Liu, X.; Kim, J.-S.; Wu, J.; Eisenberg, A. Bowl-shaped aggregates from the self-assembly of an amphiphilic random copolymer of poly(styrene-co-methacrylic acid). *Macromolecules* **2005**, *38*, 6749–6751
- (49) Riegel, I. C.; Eisenberg, A. Novel bowl-shaped morphology of crew-cut aggregates from amphiphilic block copolymers of styrene and 5-(*N*, *N*-diethylamino)isoprene. *Langmuir* **2002**, *18*, 3358–3363.
- (50) Sun, H.; Liu, D.; Du, J. Nanobowls with controlled openings and interior holes driven by the synergy of hydrogen bonding and  $\pi$ - $\pi$  interaction. *Chem. Sci.* **2019**, *10*, 657–664.
- (51) Kim, K. T.; Zhu, J.; Meeuweissen, S. A.; Cornelissen, J. J. L. M.; Pochan, D. J.; Nolte, R. J. M.; van Hest, J. C. M. Polymersome stomatocytes: Controlled shape transformation in polymer vesicles. *J. Am. Chem. Soc.* **2010**, 132, 12522–12524.
- (52) Wilson, D. A.; Nolte, R. J. M.; van Hest, J. C. M. Autonomous movement of platinum-loaded stomatocytes. *Nat. Chem.* **2012**, *4*, 268–274.
- (53) Wang, X.; Figg, C. A.; Lv, X.; Yang, Y.; Sumerlin, B. S.; An, Z. Star architecture promoting morphological transitions during polymerization-induced self-assembly. *ACS Macro Lett.* **2017**, *6*, 337–342.